ISBN: 978-3-95450-231-8 ISSN: 2673-5490 doi: 10.18429/JACoW-IPAC2023-TUPA132

ULTRA THIN Cs_3Sb PHOTOCATHODES WITH ANOMALOUSLY HIGH QUANTUM EFFICIENCY

C.A. Pennington[1], E.M. Echeverria[1], M. Gaowei[2], J. Smedley[3], P. Saha[4], S. Karkare[4], A. Galdi[5], J. Maxson[1]
[1]Cornell University, Ithaca, NY, USA
[2]Brookhaven National Laboratory, Upton, NY, USA
[3]SLAC National Accelerator Laboratory, Menlo Park, CA, USA
[4]Arizona State University, Tempe, AZ, USA
[5]Universita degli Studi di Salerno, Fisciano (SA), Italy

Abstract

In this proceeding, we demonstrate the synthesis of epitaxial Cs_3Sb films with a high degree of crystallinity on silicon carbide substrates. Films less than 10 nm thin are grown in vacuum and exhibit percent level quantum efficiencies at 532 nm. We find a positive correlation between quantum efficiency and improved crystallinity of the photocathode film, particularly in the longer wavelengths of the visible spectrum. We present a model describing the optical interference effects observed in the SiC - Si substrate multilayer that enhance quantum efficiency of the thin film photocathodes by almost a factor of two at particular wavelengths. Additionally, we characterize the surface and bulk crystallinity of epitaxial Cs_3Sb films using both X-ray diffraction (XRD) and reflection high energy electron diffraction (RHEED) in an endeavor to identify relationships between crystalline phases and photocathode performance.

INTRODUCTION

Thin film alkali antimonide photocathodes are high-efficiency photo-emitting sources for electron accelerators and photon detectors. To date, all alkali antimonide photocathodes used as electron sources in actual accelerators are polycrystalline and disordered. Low roughness and high quantum efficiency (QE) directly correlate to improved electron beam brightness at the cathode, and are characteristic parameters of alkali antimonide photocathodes [1], such as Cs_3Sb which has conventionally been grown in polycrystalline form until a recent experiment demonstrated the synthesis of single-crystal films using molecular beam epitaxy (MBE). [2] These findings motivated our experiments to identify correlations between the photoemission properties of epitaxial Cs_3Sb with the crystallinity of the material. Investigating ordered, smooth, and high QE cathodes now appears to be a path to higher brightness electron beams.

EXPERIEMENTAL DETAILS

In-operando XRD, XRF, XRR, and RHEED with *in-situ* QE measurements were performed on Cs_3Sb photocathode films at the National Synchrotron Light Source II (NSLS-II) Beamline 4-ID ISR. Photocathodes were grown in a custom growth chamber equipped with the tools listed above to perform each measurement in-vacuum. [3] The growth chamber was mounted in the hutch at the end of the beamline on a motorized rotation stage. Beryllium windows allow the 11.5 keV x-rays to enter the chamber, interact with the film, and exit the chamber onto Eiger 1M detectors and a fluorescence detector. Real-time thickness and stoichiometry measurements of the film during the growth were performed with x-ray reflectivity and fluorescence. XRD scans were performed intermittently for each sample at approximately every 3 nm deposited.

The cathode growth chamber was maintained at a pressure of 1×10^{-9} Torr during film deposition. Two growth techniques used in these experiments were pulsed laser deposition (PLD) and thermal evaporation. The PLD method starts with a pulsed UV excimer laser blasting a solid Sb target chamber in the growth to vaporize the material onto a mounted substrate. An in vacuum resistive heating cell was used to evaporate Sb in the thermal evaporation case. A similar resistive heating cell was used to evaporate Cs into the chamber for both growth techniques. We used 3C-SiC(100) and graphene-bilayer coated 4H-SiC(001) as substrates for the growth. Substrates were cleaned with IPA and methanol sonication and degassed in the vacuum chamber at over 500°C. Substrates were held at temperatures above 80°C during growth. XRD, RHEED, XRF, and XRR scans were done *in-operando* and after the photocathode layer was complete.

Similar RHEED and quantum efficiency measurements were performed in the PHOEBE lab at Cornell University and are also presented in this proceeding. Thin film Cs_3Sb photocathode were grown on 3C-SiC(100) via molecular beam epitaxy (MBE). Streaky RHEED patterns indicative of smooth, flat surfaces were seen with most photocathode samples, and most film thicknesses were less than 10 nm. QE and RHEED results are consistent between both facilities.

RESULTS AND DISCUSSION

Spectral Response

A monochromator light source was used for spectral response and QE measurements of the photocathode films

ISBN: 978-3-95450-231-8 ISSN: 2673-5490 doi: 10.18429/JACoW-IPAC2023-TUPA132

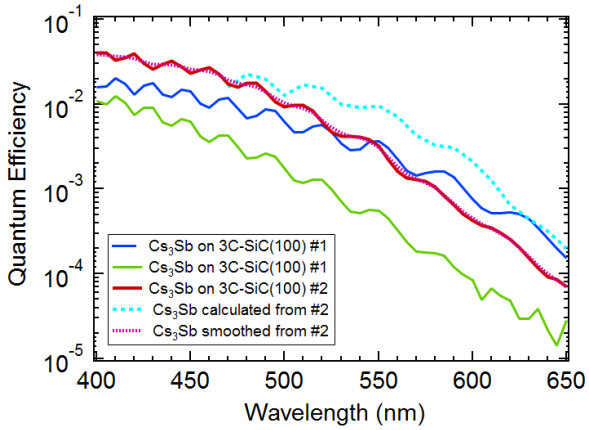

Figure 1: Oscillations are induced by thin film interference in the photocathode-substrate multilayer. The blue and green curves correspond to two different films grown on the same substrate. The red curve corresponds to a film grown on an entirely different substrate, and the dashed light blue curve represents an estimate of the oscillation period from a thin film interference model.

shown in Fig. 1. Optical interference in the photocathode-substrate multilayer Fig. 2 is responsible for the oscillations observed in the spectral response. We solve for the reflectance R_f, transmittance T_f, and absorptance A_f of the thin film system using the transfer matrices assuming nearly normal incidence:

$$A = \begin{bmatrix} a_{11} & a_{12} \\ a_{21} & a_{22} \end{bmatrix} = \begin{bmatrix} \frac{1}{2} & \frac{1}{2} \\ \frac{1}{2} & -\frac{1}{2} \end{bmatrix} M_1 M_2 M_3 \begin{bmatrix} 1 & 0 \\ n_3 & 0 \end{bmatrix} \quad (1)$$

$$M_i = \begin{bmatrix} \cos\beta_i & -\frac{i\sin\beta_i}{n_i} \\ -in_i\sin\beta_i & \cos\beta_i \end{bmatrix} \quad (2)$$

where β_i is the propagation constant $\frac{2Pi}{\lambda} n_i d_i n_i$, n_i is the index of refraction, d_i is the thickness of the ith layer, $A_f = 1 - R_f - T_f$ is the absorptance, $R_f = |\frac{1}{a_{11}}|^2$ is the reflectance, and $T_f = |\frac{a_{21}}{a_{11}}|^2$ is the transmittance. Multiplying this absorptance by a smooth, non-oscillating spectral response curve yields the dashed blue curve in Fig. 1. Although the nominal QE values from the dashed blue curve are qualitative, the behavior shows that the frequency of oscillations matches the data (solid curve), confirming that oscillations are due to thin film interference. Two of the curves shown in Fig. 1 (green, blue) are measurements from films grown on the same SiC layer which is different from the red curve. The photocathode film was grown on the substrate, QE data was collected, then the film was burned off for the second growth. The offset in the periodicity of these curves compared to the red curve is due to the two substrates having slightly different SiC layer thicknesses. The 3C-SiC(100) layers are grown epitaxially on Si(100) by MTI Corp. The nominal substrate thickness of the SiC is 1.3 µm, and the 0.02 µm difference in thickness corresponding

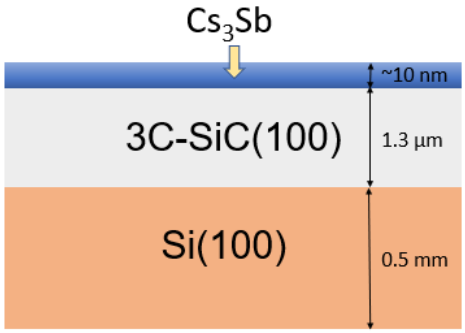

Figure 2: A substrate used in this experiment is 3C-SiC(100), which is grown epitaxially on Si(100). The 3C-SiC(100) layer is 1.3 µm thick.

to the observed offset in oscillation periodicity is within the variability of the thickness from the manufacturer.

An interesting feature of the oscillations in the spectral response is that the QE modulates by up to a factor of two between wavelengths that are about 20 nm apart. For example, in Fig. 1, the ratio of the QE at 480 nm and 508 nm from the blue curve is 2. The QE then increases to a relative maximum again at 524 nm, and is greater than $\frac{3}{4}$ of the QE at 480 nm. It is important to recognize this feature if thin photocathodes grown on 3C-SiC are going to be employed in photoinjectors in order to select an ideal wavelength for the drive laser to match with a relative maximum in the oscillation. The advantage of ultra thin films (<10 nm) is the reduced roughness discussed in following sections and the relatively high QE.

An explanation for the large modulations in the spectral response can be found by estimating the electron escape probability from the film with inspiration from the work in [4]. The total absorption of the photocathode layer can be determined by calculating the forward and backward travelling components of the electric field in the film:

$$E_y = E_o e^{i\omega t}\left(c_f e^{i\bar{n}_{\mathrm{PC}} kx} + c_b e^{-i\bar{n}_{\mathrm{PC}} kx}\right) \quad (3)$$

where c_f and c_b are the coefficients of the forward and backward travelling waves and n_{PC} is the complex index refraction of the photocathode film. We solve the for coefficients c_f and c_b by applying boundary conditions for the electric field in the multilayer. We then calculate the net power density flow into the material from the Poynting vector $(S_x) = 1/2 E_y \cdot H_z^*$, where H_z^* is the complex conjugate of the magnetic field in the material which can be derived from $H = (-1/\mu)\int \nabla X E dt$. A quantity for the differential power density can then be defined as $P_a = \nabla \cdot \mathrm{Re}\,(S_x)$. The power absorption profile $a(x)$ in the photocathode film is then equal to the differential power density throughout the film divided by the input power at the surface: $a(x) = P_a / P_{\mathrm{in}}$. Where the input power can be calculated from:

$$P_{\mathrm{in}} = -\left(\frac{k n_{\mathrm{vac}}}{2\omega\mu_o\mu_V}\right)|E_o|^2 . \quad (4)$$

ISBN: 978-3-95450-231-8 ISSN: 2673-5490 doi: 10.18429/JACoW-IPAC2023-TUPA132

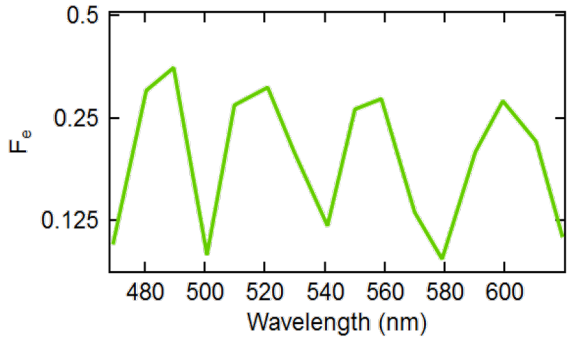

Figure 3: The single electron escape probability calculated over a range of visible wavelengths. The calculation was performed using available optical constants for the PC-substrate multilayer.

Once the absorption profile $a(x)$ is calculated, we can estimate the escape probability of a single electron from the photocathode film by

$$F_e = \int_0^h a(x) e^{-(x/\lambda_{esc})} dx \quad (5)$$

where h is the thickness of the photocathode layer, λ_{esc} is the characteristic escape depth of the material, which is approximately λ_{esc}=220 nm for Cs_3Sb. [5]. The electron escape probability (F_e) for a range of visible wavelengths is plotted in Fig. 3 using optical constant for the three thin film layer. We find that the escape probability oscillates at almost the exactw frequency as the QE in the spectral response. Since the value for the electron escape depth of Cs_3Sb is not well known, the nominal values for the escape probability are considered qualitatively for this result. However, the ratio of F_e values at the maxima, corresponding to net constructive interference, are approximately a factor of 3 larger than the values at the minima corresponding to net destructive interference. This factor of 3 between the escape probability minima and maxima is large enough to account for the modulations in the spectral response.

Crystal Structure - XRD and RHEED

RHEED images are shown in Fig. 4 for (a) graphene-coated 4H-SiC(001) and (b) 3C-SiC(100). The corresponding RHEED images from the Cs_3Sb photocathode films are shown below the substrate. Several samples grown at 90°C using both the PLD and thermal evaporation techniques exhibit long streaks in the RHEED pattern, indicative of flat, smooth surfaces. Azimuthal RHEED scans are shown in Fig. 4 as the samples are rotated on a motorized stage in the growth chamber. Several samples have RHEED patterns with aziumthal dependence which implies a preferred in-plane crystal orientation and epitaxial coordination with the substrate. Preliminary results from XRD scans and RHEED are consistent with lattice matches between the photocathode film and substrate. The thin film alkali antimonide photocathodes grown on 3C-SiC(100) substrates offer major advantages for bright electron beams in the form of reduced roughness and high QE. Optical interference in the film layers pose another potential advantage in the form of increased QE, provided the silicon carbide substrate thickness is tuned to give constructive interference at the desired drive laser wavelength.

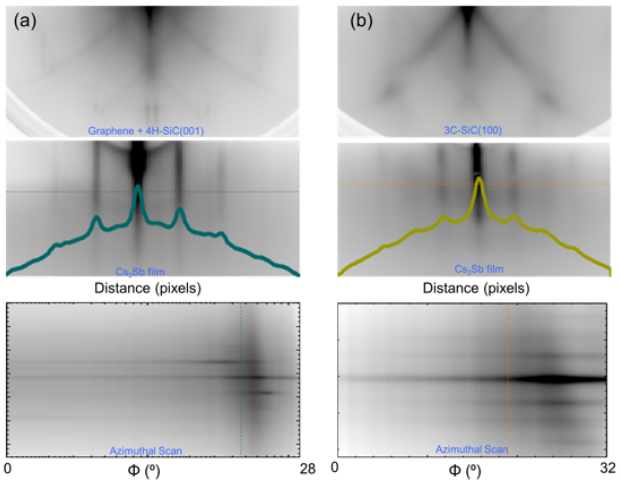

Figure 4: RHEED patterns from Gr/4H-SiC(001) and 3C-SiC(100) substrates are shown in (a) and (b) respectively. The Cs_3Sb film is shown below, with long streaks suggesting a flat surface. Azimuthal scans are shown in the bottom set of images, revealing angular dependence in the orientation of the film grown the 4H-SiC(100).

REFERENCES

[1] Jun Feng *et al.*, "Near atomically smooth alkali antimonide photocathode thin films"', *J. Appl. Phys.*, vol. 121, no. 4, p. 044904, 2017. doi:10.1063/1.4974363

[2] C.T. Parzyck, A. Galdi, *et al.*, *Phys. Rev. Lett.*, "Single-Crystal Alkali Antimonide Photocathodes: High Efficiency in the Ultrathin Limit", vol. 128, p. 114801, 2022. doi:10.1103/PhysRevLett.128.114801

[3] M. Gaowei *et al.*, "Synthesis and x-ray characterization of sputtered bi-alkali antimonide photocathodes", *Appl. Phys. Lett.*, vol. 5, no 11, p. 116104, 2017. doi:10.1063/1.5010950

[4] A. Alexander *et al*, "Enhanced photocathode performance through optimization of film thickness and substrate", *J. Vac. Sci. Technol., B*, vol. 35, p. 022202, 2017. doi.org/10.1116/1.4976527

[5] P.D. Townsend *et al.*, *J. Phys. D: Appl. Phys.*, "Designs for waveguide and structured photocathodes with high quantum efficiency", vol. 39, p. 1525, 2006. doi:10.1088/0022-3727/39/8/012